Heating conversion of indole-3-carbinol into *N*-substituted oligomers with anti-melanoma effect

Jia Cheng Qian [1], Heng Peng Zhang [1], Yi Wang, Dan Liu [*]

State Key Laboratory Cultivation Base for TCM Quality and Efficacy, Nanjing University of Chinese Medicine, Nanjing 210023, PR China

ARTICLE INFO

ABSTRACT

Cruciferous vegetables (CVs) are globally consumed with some health benefits believed to arise from indole-3-carbinol (I3C), a labile phytochemical liberated from indole glucosinolates, but few reports describe the effect of cooking on I3C reactions. Here, we present heat-promoted direct conversions of I3C in broccoli florets into indole derivatives, which are unique in the *N*-indolylmethylation and -hydroxymethylation of indole nuclei by 3-methyleneindole and formaldehyde formed in situ from the I3C dehydration and the dimerization of I3C to 3,3′-diindolylmethane (DIM), respectively. Such *N*-substituted indoles were found in a range of 0.4–4.6 μg per gram of steamed broccoli florets, with a novel compound *N*-(indol-3-ylmethyl)-3,3′-diindolylmethane (DIM-1) bio-evaluated to inhibit A375 cells with an IC_{50} value of 1.87 μM. In aggregation, the investigation discloses the promoting effect of heating on the I3C transformation in CVs and identifies DIM-1 as an anti-cancer drug candidate, and thus updates the knowledge of I3C and bioactive derivatives thereof.

1. Introduction

Cruciferous vegetables (CVs), including broccoli, cauliflower, kale, collard, turnip, mustard greens, and cabbage, are ones of the most popular and widely cultivated vegetables in the world (Johnson, 2018; Li et al., 2022). Daily ingestion of CVs offers various nutrients and health-promoting substances (Lee, Liang, Stuckey, & Hu, 2023; Lyles et al., 2021). CVs belong to the Brassicaceae family and being recognized for their richness in sulfur-containing glucosinolates (GSLs) (Blažević et al., 2020; Dong et al., 2021). Among the ~30 GSLs typically present in CVs, the tryptophan-derived indole glucosinolates (IGs) have received substantial attention due to their potential cancer-preventive effect (Mikkelsen et al., 2012). However, native GSLs possess little biological activity. To fulfil most of their functions, they need to be activated by myrosinases to hydrolyze the glucose residue (Blažević et al., 2020). As for IGs, the hydrolysis reaction produces thiohyndroximate-O-sulfonate, which is spontaneously decomposed into thiocyanate ion and indole-3-carbinol (I3C) (Nagia, Morgan, Gamel, & Farag, 2023).

CVs-derived I3C was considered as a "star molecule" for regulating some biological processes in mammals and, particularly, exerting cancer-preventive action in diverse models (Gronke et al., 2019; Lee et al., 2019). However, I3C is chemically labile and can be rapidly metabolized in vivo within 1 h after ingestion (Anderton et al., 2004), which suggests the health benefit of I3C intakes might arise from its metabolites. In our previous work, we reported the post-ingestion conversion of I3C in gastrointestinal tracts (Lin et al., 2022). Generally, in acidic contexts (e.g., gastrointestinal tracts of mammals and ionic liquid), I3C is apt to dehydrate to give a salt, 3-methyleneindolium (3MI-s) (Lin et al., 2022; Liu et al., 2021). Chemically, 3MI-s is reactive enough to play an indispensable role in the I3C transformation into cancer-preventive indole oligomers, such as: DIM (3,3′-diindolyl-methane), LTr1 (2-(indol-3-ylmethyl)-3,3′-diindolylmethane), and CTr (5,6,11,12,17,18-hexahydrocyclononal[1,2-b:4,5-b':7,8-b″]triindole) (Lin et al., 2022; Liu et al., 2021). During the production of kimchi via the fermentation of cruciferous vegetable with acid-produced bacterium, I3C could converse into high-order indole oligomers (Qian, Liu, Lin, Zhu, & Tan, 2022). Among which, the linear tetramer of I3C (LTet) (2-((1H-indol-3-yl)methyl)-3-((3-((1H-indol-3-yl)methyl)-1H-indol-2-yl)methyl)-1H-indole) is substantially toxic to acute myeloid leukaemia (AML) cells.

In view of this and other benefits (Johnson, 2018; Li et al., 2022; Lyles et al., 2021), CVs have been recommended by the 2015–2020 Dietary Guidelines to consume each day because the daily CV ingestion is evidenced to make their health-promoting effects more pronounced

and long-lasting (Choe, Yu, & Wang, 2018). Before ingested, CVs are often cooked in different ways such as boiling, blanching, steaming and stir-frying, where the heating process is inevitable (Barnum, Cho, Markel, & Shih, 2024). On the other hand, the glucosinolate constituents in CVs are generally thermolabile and can decompose into diverse daughter molecules upon being heated or cooked (Sun et al., 2021). Therefore, thermal breakdown of IGs had been widely investigated. For example, after exposure to heat treatment, IGs could either decompose into thiocyanate ion and indoleacetonitriles (Niels, Martin, & Jae, 2009), or provide a new minor indole condensation product corresponding to a 3-(indolylmethyl)glucobrassicin (Chevolleau, Debrauwer, Boyer, & Tulliez, 2002). However, the chemistry governing the heat-promoted conversion of I3C remains poorly investigated. Inspired by the thermal dehydration of amino acids (Xu et al., 2022) and conjugation system-eased reactions (Wen, Yang, Deng, & Chen, 2023), we were increasingly curious about whether, and if yes, how I3C in CVs undergoes heat-promoted reaction(s). Herein, we present the heat-promoted direct conversion of I3C in broccoli florets into indole derivatives which are structurally unique in the *N*-indolylmethylation or –hydroxymethylation of the imine group of indole nuclei. Among such *N*-alkylated indoles was *N*-(indol-3-ylmethyl)-3,3′-diindolylmethane (DIM-1) which was demonstrated to show anti-proliferation effect and present at 3.1 µg/g of steamed CVs. Collectively, the work unravels the heat-promoted conversion of I3C (derived from indole glucosinolates in CV tissues) and identifies DIM-1 as an anti-cancer drug candidate, and thus updates the knowledge about I3C as well as its source plants (or CVs) and bioactive derivatives.

2. Materials and methods

2.1. Reagents and materials

I3C (C_9H_9NO, ≥98%), IAld (indole-3-aldehyde, C_9H_7NO, ≥98%), DIM ($C_{17}H_{14}N_2$, ≥98%), [EMIm][Cl] (1-ethyl-3-methylimidazolium chloride, $C_6H_{11}ClN_2$, ≥98%) were purchased from Aladdin Chemical Co. (Shanghai, China), and gastric juice from Solarbio (Beijing, China). CTr ($C_{27}H_{21}N_3$) and LTr1 ($C_{26}H_{21}N_3$) were synthesized as reported (Lin et al., 2022; Liu et al., 2021). Petroleum ether, dichloromethane, ethyl acetate, and methanol were supplied by Aladdin Chemical Co. (Shanghai, China), and acetonitrile by Merck (Burlington, USA). Ultrapure water was produced by MilliQ purification system from Merck (France).

2.2. Sampling and analysis of broccoli florets

As reported earlier (Qian et al., 2022), fresh broccoli florets were purchased from super market in Nanjing, and three subsamples flesh broccoli florets (ca. 100 g) of the homogeneous batch (ca. 1 kg) were treated and analyzed. Each portion was cut into small pieces and heated by steam (100–105 °C) for 10 min. After cooling, the vegetable material was ground and homogenized for 5 min. And then, the liquid-liquid extraction of I3C-related derivatives was conducted, in which the pretreated sample was added in distilled water (50 mL), and extracted with dichloromethane (50 mL × 3 times). After being concentrated to 5 mL, the combined organic layer was dried with anhydrous Na_2SO_4, followed by filtration over nylon syringe filter (0.45 µm). A 2-µL aliquot of the filtrate was taken for analysis using high performance liquid chromatography (HPLC) coupled to high-resolution mass spectrometry (HRMS). All the HPLC-HRMS parameters used for analysis are displayed in Table S2.

2.3. Identification of heat-promoted condensation products of I3C

I3C (2 mmol) was added to a Schlenk pressure tube, and heated at 100 °C till the solid material melting completely. After being stirred for 10 min, the mixture was cooled to ambient temperature and successively chromatographed over Preparative RP-HPLC (reverse phase-high performance liquid chromatography) with an acetonitrile-water gradient. Specifically, preparative RP-HPLC was performed on an Agilent Technologies 1260 Infinity LC System using an Agilent Eclipse XDB-C18 column (5 µm, 10 × 250 mm). In the purification process, the reaction residue was dissolved in acetonitrile (1 mL), and 20-µL aliquot of the sample was injected in RP-HPLC. With isocratic elution of acetonitrile/ H_2O (v/v = 70:30), 7 main components were collected. By evaporating of solvent under 35 °C, the dry compounds were obtained for identification. By comparing their spectrophotometry and HPLC data with our previous work (Lin et al., 2022; Liu et al., 2021; Qian et al., 2022), 3,3′-diindolylmethane (DIM, 23.0 mg), 2-(indol-3-ylmethyl)-3,3′-diindolylmethane (LTr1, 11.8 mg), 5,6,11,12,17,18-Hexahydrocyclononal[1,2-b:4,5-b':7,8-b"]-triindole (CTr, 5.4 mg), *N*-(indol-3-ylmethyl)-3,3′-diindolylmethane (DIM-1, 7.5 mg), *N*-(indol-3-ylmethyl)-indole-3-carbaldehyde (IAld-1, 4.6 mg), *N*-(indol-3-ylmethyl)-indole-3-carbinol (I3C-1, 8.9 mg), and *N*-hydroxymethyl-3,3′-diindolylmethane (DIM-2, 7.8 mg) were identified.

2.4. The oligomerization of I3C under artificial gastric juice

To a round-bottom flask preloaded with artificial gastric juice (95 ml) was added dropwise with I3C (1 g dissolve in 5 ml DMSO). The resulting mixture was stirred at 37 ± 2 °C for 1 h, and quenched by a saturated aqueous $NaHCO_3$. Followed by the extract of the reactant solution with EtOAc (3 × 100 ml), the combined organic layer was washed with brine (100 ml), dried over Na_2SO_4 and concentrated in vacuo. The crude product was dissolved in acetonitrile for the HPLC-HRMS analysis.

2.5. The synthesis of N-substituted oligomers of I3C

All NMR spectra were acquired on a Bruker AV-500 spectrometer using TMS as an internal standard with ^{1}H and ^{13}C nuclei observed at 500 and 125 MHz, respectively. The chemical shift was recorded relative to the solvent acetone-d_6 (δ_H 2.05 and δ_C 29.8).

2.5.1. Synthesis of N-hydroxymethylated indoles

(1) General method (Scheme S1): A mixture of indole (1 eq), Cs_2CO_3 (1.1 eq for each N site), and polyformaldehyde (1.3 eq) in 1,4-dioxane was added into a Schlenk flask (25 mL) and stirred at room temperature until the reaction was completed. After the reaction, the mixture was diluted with ethyl acetate, washed with water for 3 times, and concentrated in vacuo. Finally, the reaction mixture was purified by silica gel (100–200 mesh) column chromatography to afford *N*-hydroxymethyl-indoles.

(2) *N*-hydroxymethyl-indole-3-carbinol (I3C-2): ^{1}H NMR (500 MHz, acetone-d_6) δ 7.67 (dt, J = 7.9, 0.9 Hz, 1H), 7.52 (dt, J = 8.2, 0.9 Hz, 1H), 7.28 (s, 1H), 7.20–7.17 (m, 1H), 7.10–7.07 (m, 1H), 5.62 (d, J = 7.3, 2H) and 3.79 (t, J = 5.5 Hz, 1H). ^{13}C NMR (125 MHz, acetone-d_6) δ 136.5, 128.1, 126.1, 121.5, 119.24, 119.22, 116.7, 109.9, 69.0 and 56.1.

(3) *N*-hydroxymethyl-indole-3-carboxaldehyde (IAld-2): ^{1}H NMR (500 MHz, acetone-d_6) δ 10.02 (s, 1H), 8.24 (d, J = 7.9 Hz, 1H), 8.22 (s, 1H), 7.69 (d, J = 8.2 Hz, 1H), 7.37–7.34 (m, 1H), 7.32–7.28 (m, 1H), 5.89 (dd, J = 8.2, 7.6 Hz, 1H) and 5.80 (d, J = 7.6 Hz, 2H). ^{13}C NMR (125 MHz, acetone-d_6) δ 184.5, 139.5, 137.0, 125.6, 123.8, 122.7, 121.6, 118.5, 111.1 and 70.2.

(4) *N*-hydroxymethyl-3,3′-diindolylmethane (DIM-2): ^{1}H NMR (500 MHz, acetone-d_6) δ 9.94 (br, 1H), 7.61 (t, J = 7.8 Hz, 2H), 7.50 (d, J = 8.2 Hz, 1H), 7.40 (d, J = 8.2 Hz, 1H), 7.17–7.09 (m, 4H), 7.04 (dt, J = 7.5, 0.7 Hz, 1H), 6.99 (dt, J = 7.5, 0.7 Hz, 1H), 5.59 (d, J = 7.3 Hz, 2H) and 5.29 (t, J = 7.3 Hz, 1H). ^{13}C NMR (125 MHz, acetone-d_6) δ 137.0, 136.6, 128.9, 127.7, 125.8, 122.7, 121.3, 121.1, 119.0, 118.9, 118.8, 118.4, 115.3, 114.6, 111.2, 109.9, 69.0 and 20.8.

(5) *N*,*N*′-dihydroxymethyl-3,3′-diindolylmethane (DIM-4): [1]H

NMR (500 MHz, acetone-d_6) δ 7.61 (dt, $J = 7.9$, 0.8 Hz, 2H), 7.51 (dt, $J = 7.9$, 0.8 Hz, 2H), 7.18–7.15 (m, 2H), 7.12 (s, 2H), 7.06–7.03 (m, 2H), 7.59 (d, $J = 7.3$ Hz, 4H), 5.34 (t, $J = 7.3$ Hz, 2H) and 4.20 (s, 2H). ^{13}C NMR (125 MHz, acetone-d_6) δ 136.5, 128.8, 125.8, 121.3, 119.00, 118.97, 114.9, 109.9, 69.0 and 20.6.

2.5.2. Synthesis of N-hydroxymethylated indoles

Following Scheme 1, IAld-1, I3C-1, DIM-1, and DIM-3 were obtained successfully.

(1) *N*-(indol-3-ylmethyl)-indole-3-carbaldehyde (IAld-1): A 10 mL Schlenk tube containing a magnetic stir bar was added successively with I3C (5 mmol, 1.0 equiv), IAld (10 mmol, 2.0 equiv), and [EMIm][Cl] (2.5 mmol, 0.5 equiv). The mixture was stirred for 5 min at room temperature. Then, the tube was sealed and heated to 120 °C for 1 h. Afterwards, the mixture was cooled to room temperature and diluted with ethyl acetate. The organic layer was washed with water for 3 times, dried over Na$_2$SO$_4$ and concentrated in vacuo. Finally, the reaction mixture was purified by silica gel (SiO$_2$, 100–200 mesh) column chromatography (dichloromethane/MeOH, 200:1, v/v) to afford the IAld-1 (645 mg, 47% yield, R$_f$ = 0.5 (DCM/MeOH, 200:1)). ^{1}H NMR (500 MHz, acetone-d_6) δ 10.41 (br, 1H), 9.95 (s, 1H), 8.24 (d, $J = 7.8$ Hz, 1H), 8.16 (s, 1H), 7.78 (d, $J = 8.2$ Hz, 1H), 7.61 (d, $J = 2.6$ Hz, 1H), 7.56 (dd, $J = 8.0$, 0.8 Hz, 1H), 7.46 (d, $J = 8.2$ Hz, 1H), 7.32 (dt, $J = 7.6$, 1.3 Hz, 1H), 7.27 (dt, $J = 7.5$, 1.1 Hz, 1H), 7.15 (dt, $J = 7.6$, 1.1 Hz, 1H), 7.02 (dt, $J = 7.5$, 1.0 Hz, 1H), 5.70 (s, 2H). ^{13}C NMR (125 MHz, acetone-d_6) δ 183.9, 139.3, 137.6, 137.0, 126.6, 125.6, 125.2, 123.4, 122.3, 121.9, 121.6, 119.5, 118.3, 117.9, 111.7, 111.0, 109.8, 42.3.

(2) *N*-(indol-3-ylmethyl)-indole-3-carbinol (I3C-1): IAld-1 (274 mg, 1 eq) was dissolved in a mixture solution of MeOH/THF (v:v = 1:1, 5 mL). After cooled to 0 °C, NaBH$_4$ (114 mg, 3 eq) was added to the mixture in portions during a period of 30 min. The reacting mixture was stirred for another 2 h, and being diluted with ethyl acetate, washed with water for 3 times, and concentrated in vacuo. Finally, the reaction mixture was purified by silica gel (100–200 mesh) column chromatography to afford I3C-1 (257 mg, 93%). ^{1}H NMR (500 MHz, acetone-d_6) δ 10.27 (br, 1H), 7.67 (dt, $J = 7.9$, 0.9 Hz, 1H), 7.62 (dt, $J = 7.9$, 0.9 Hz, 1H), 7.54 (dd, $J = 8.0$, 0.9 Hz, 1H), 7.43–7.41 (m, 2H), 7.29 (s, 1H), 7.18–7.15 (m, 1H), 7.13–7.10 (m, 1H), 7.06–7.03 (m, 1H), 7.01–6.98 (m, 1H), 5.52 (s, 2H), 4.77 (dd, $J = 5.5$, 0.6 Hz, 2H) and 3.69 (t, $J = 5.5$ Hz, 1H). ^{13}C NMR (125 MHz, acetone-d_6) δ 137.9, 136.9, 127.7, 126.8, 126.4, 124.3, 121.6, 121.2, 119.2, 119.1, 118.62, 118.59, 115.8, 111.7, 111.5, 109.8, 56.2 and 41.1.

(3) *N*-(indol-3-ylmethyl)-3,3′-diindolylmethane (DIM-1): To a solution of indole (117 mg, 2 eq) and SiO$_2$ (200 mg) in DCM (2 mL) was added I3C-1 (69 mg, 1 eq) at 0 °C. After stirred for 1 h at rt., the reacting mixture was filtered to remove SiO$_2$. Ice-cooled water and DCM was added to the filtrate, and the organic layer was collected. Followingly, the organic layer was washed with water, dried with Na$_2$SO$_4$, and concentrated under reduced pressure. After purification by flash column chromatography, DIM-1 (67 mg) was obtained in 72% yield. ^{1}H NMR (500 MHz, acetone-d_6) δ 10.18 (br, 1H), 9.90 (br, 1H), 7.58–7.55 (m, 3H), 7.49 (d, $J = 8.0$ Hz, 1H), 7.40 (dd, $J = 8.2$, 0.9 Hz, 1H), 7.38–7.36 (m, 2H), 7.21 (s, 1H), 7.12–7.06 (m, 4H), 6.99–6.94 (m, 3H), 5.51 (s, 2H) and 4.21 (d, $J = 1.0$ Hz, 2H). ^{13}C NMR (125 MHz, acetone-d_6) δ 137.00, 136.98, 136.9, 128.5, 127.7, 126.8, 126.3, 124.0, 122.6, 121.6, 121.1, 120.9, 119.13, 119.07, 118.9, 118.8, 118.3, 118.2, 115.0, 114.0, 112.0, 111.4, 111.2, 109.8, 41.4 and 21.1.

(4) *N,N*′-bis(indol-3-ylmethyl)-DIM (DIM-3): I3C-1 (69 mg, 1 eq) and SiO$_2$ (200 mg) was suspended in DCM (2 mL) at 0 °C, and being stirred for 1 h at rt. After being filtered to remove SiO$_2$, ice-cooled water and DCM was added to the filtrate, and the organic layer was collected. Followingly, the organic layer was washed with water, dried with Na$_2$SO$_4$, and concentrated under reduced pressure. After purification by flash column chromatography, DIM-3 (42 mg) was obtained in 67% yield. ^{1}H NMR (500 MHz, acetone-d_6) δ 10.17 (br, 2H), 7.53 (d, $J = 9.0$ Hz, 4H), 7.47 (dd, $J = 8.0$, 0.7 Hz, 2H), 7.39 (d, $J = 8.2$ Hz, 2H), 7.34 (d, $J = 2.5$ Hz, 2H), 7.17 (s, 2H), 7.11–7.08 (m, 4H), 6.98–6.92 (m, 4H), 5.47 (d, $J = 0.4$ Hz, 4H) and 4.17 (s, 2H). ^{13}C NMR (125 MHz, acetone-d_6) δ 137.0, 136.9, 128.4, 126.8, 126.3, 124.0, 121.6, 120.9, 119.2, 119.1, 118.8, 118.2, 114.0, 112.0, 111.4, 109.8, 41.4 and 21.1.

2.6. Preparation of stock solutions

Stock solution of *N*-substituted derivatives of I3C were dissolved in acetonitrile (1000 mg/L) and stored in dark glass containers at −4 °C. As for analysis, the working standard solution were prepared daily by dilution with acetonitrile.

2.7. Cell proliferation assay

Human A375 melanoma cells (Procell Life Science & Technology Co., Ltd., China) were seeded in 96-well plates (ca. 5000 cells per well) and cultured in the DMEM (Dulbecco's Modified Eagle Medium) media at 37 °C in a humidified atmosphere with 5% CO$_2$ supplemented with
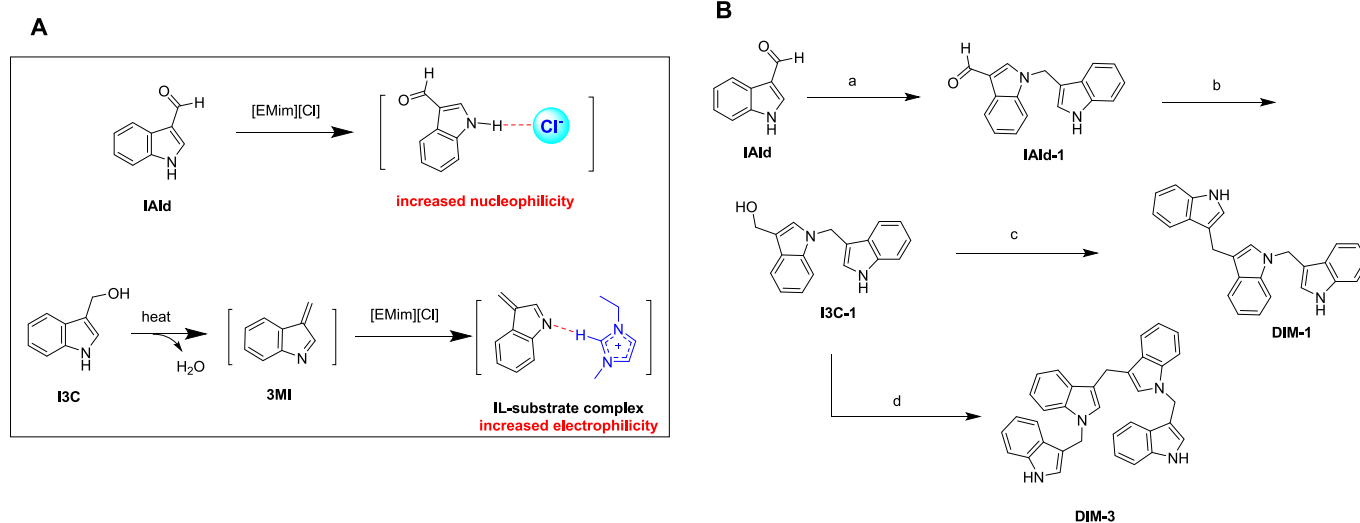
Scheme 1. Synthesis of *N*-(indol-3-yl)-methyl oligomers. (A) Ionic liquid facilitated synthetic strategy. (B) The synthesis pathway of *N*-(indol-3-yl)-methyl oligomers*

*Reagents and conditions: (a) indole-3-carbinol, [EMIm][Cl], 120 °C, 47%. (b) NaBH$_4$, MeOH, THF, rt., 93%. (c) indole, SiO$_2$, rt., 72%. (d) SiO$_2$, rt., 67%.

10% (*v*/v) fetal bovine serum (FBS, Invitrogen, USA) and 1% (v/v) penicillin-streptomycin (Yeasen Biotechnology Co. Ltd., Shanghai, China) overnight. All test compounds (I3C, I3C-1, I3C-2, IAld, IAld-1, IAld-2, DIM, DIM-1, DIM-2, DIM-3, DIM-4, and LTr1) were dissolved in DMSO at a final concentration of 10 mM as stock solution, followed by diluting with DMEM (Dulbecco's modification of Eagle's medium) to 10 μM. Then cells were treated with DMSO or test compounds in a complete growth medium (DMEM) for 48 h, the same medium was added (200 μL per well) and incubated for 1 h with 0.5 mg/mL Cell Counting Kit-8 (CCK8). The number of viable cells was measured spectrophotometrically at 450 nm on a Microplate reader. The experiment was performed in triplicate on separate occasions, and the data expressed as means ± SD (*n* = 3).

2.8. Colony formation assay

At a density of 100 cells per well, A375 cells were seeded in the 12-well plates which were treated separately for 10 days with I3C (5.0 μM) and DIM-1 (0.5 μM, 1.0 μM, 2.0 μM, and 4.0 μM, respectively). The cell colony that formed was washed twice with phosphate buffer saline (PBS), fixed with methanol at room temperature, stained with 1% crystal violet for 30 min, photographed and counted using the ImageJ software. The experiment was repeated on three separate occasions, and the data expressed as means ± SD (n = 3).

2.9. Statistical analysis

Data are expressed as the mean value with the standard deviation (SD) of measurements (mean ± SD). A probability value of $p < 0.05$ was adopted as the criterion for statistical significance.

3. Results and discussion

3.1. Heat-promoted transformation of I3C in CVs

The heating process promotes the dehydration and deamination of diversely structured compounds (Xu et al., 2022), which can be further facilitated by the simultaneous elongation of conjugation systems (Wen et al., 2023). Many organic compounds are subject to air-oxidations which are more efficient at higher temperature (Kus and Misz-Kennan, 2017; Lin et al., 2015). We therefore questioned whether I3C, liberated from indolyl glucosinolate in CVs, is vulnerable to the heat-promoted transformation. The fresh broccoli florets were therefore steamed for a 10-min duration that is frequently adopted for cooking CVs. Such heat-treated materials were extracted with dichloromethane, and evaporation of solvent from the obtained extracts under reduced pressure gave the residues. Since the electrospray ionization (ESI) mass spectrometry (MS) measurements of I3C and its analogues usually give the same characteristic ion peak at *m/z* 130.0651 (fragment, $C_9H_8N^+$) arising from 3MI (Fujioka et al., 2014; Kokotou, Revelou, Pappas, & Kokotou, 2017), thus obtained residues were analyzed by liquid chromatography (LC) in tandem with ultraviolet (UV) and high-resolution ESI mass spectrometry (HRMS) (Fig. 1A, B and S1). As illustrated in Fig. 1C, various peaks gave the 3MI fragment ion although they had different retention time (R_t) and quasimolecular ions. The observation suggested that the heating procedure did accelerate the conversion of I3C into its daughter (mainly oligomerized) products.

I3C is labile and apt to be dehydrated into 3-methyleneindole (3MI) in its salt (3MI-*s*) (Lin et al., 2022; Liu et al., 2021) form in acidic contexts. 3MI-s is quite electrophilic and thus plays a decisive role in the I3C transformation into diverse indoles in the fungal culture (Lin, Yu, Shi, Zhou, & Tan, 2023) and in the gastrointestinal tract of mice (Lin et al., 2022). However, the physiological pH of broccoli florets was determined
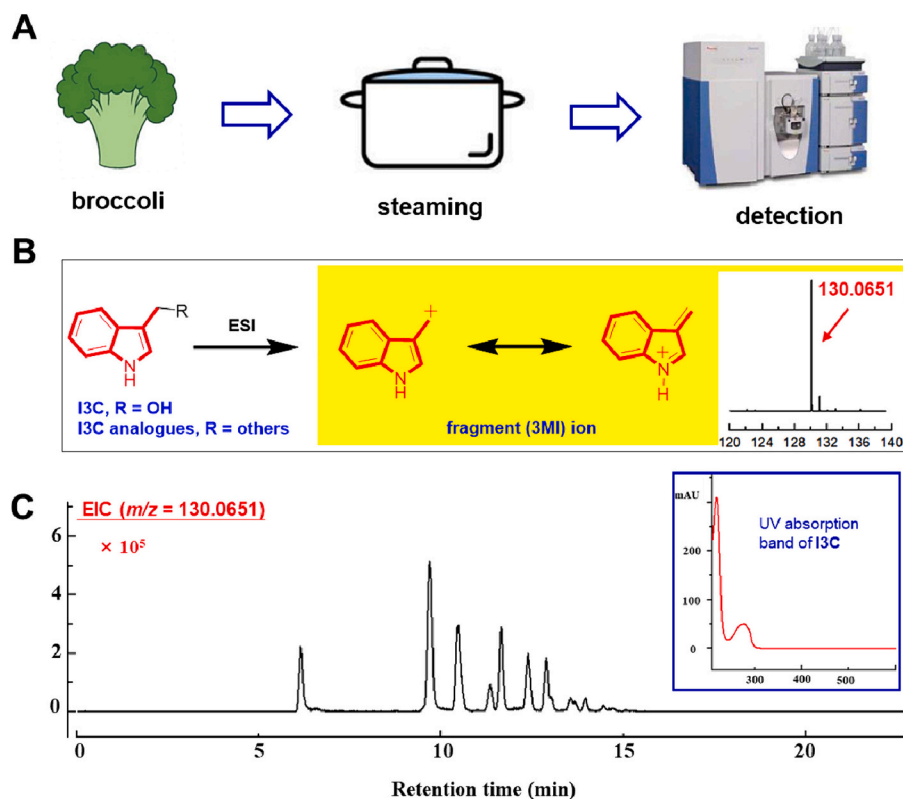
Fig. 1. Heat-promoted transformation of indole glucosinolates via I3C. (A) The flow chart illustrating the heat-promoted transformation of I3C in cruciferous vegetables (CVs). (B) The 3-methyleneindole (3MI) motif, common in molecules of I3C and its oligomers, tends to form the resonance-stabilized fragment (3-methyleneindolium) ion at *m/z* 130.0653 upon their electrospray ionization (ESI). (C) LC-UV-MS detection of indoles in steamed CVs, which gave the fragment ion at *m/z* 130.0651 and the UV absorption bands (omitted for clarity) similar to that of I3C.

to be 6.5 (Fig. S2), under which the 3MI was in its base (3MI-b) form with decreased electrophilic ability. We therefore motivated to assess the I3C conversion under heating condition at 60, 80, 100, and 120 °C. As shown in Fig. 2, after a 10-min heating, the I3C-derived products were more abundant at 100 and 120 °C than at 60 and 80 °C. Interestingly, the heat-promoted transformation pattern of I3C differed substantially from that facilitated by the gastric acid exposure which allowed mainly for its conversion into DIM, CTr and LTr1 (Fig. 2A) (Lin et al., 2022). To acquire insights into this phenomenon, a scaled-up experiment with 2 mmol of I3C was conducted under 100 °C for 10 min. The reaction mixture was purified with preparative RP-HPLC to give a total of seven compounds. By comparing the spectral data with those of standard materials (Lin et al., 2022; Liu et al., 2021; Qian et al., 2022) available in our laboratory, three compounds with R_t values being 15.569, 16.886, and 17.530 min were identified as DIM, CTr, and LTr1, respectively. With that, our curiosity was expanded to the rest four structures.

The fourth compound (R_t = 18.280 min) was demonstrated to be previously undescribed though structurally comparable to DIM (Lin et al., 2022), and for this reason and simplicity, it was termed DIM-1. However, DIM-1 was evidenced to share the same molecular formula with LTr1 ($C_{26}H_{21}N_3$) rather than DIM, from its high-resolution electrospray ionization mass spectroscopy (HRESIMS). The ^1H and ^{13}C NMR spectra of DIM-1 (Fig. S5 and S6) displayed the presence of three indole nuclei that gave typically the signal clusters arising from 15 protons at δ_H 6.50–8.50 and 24 carbons at δ_C 109.5–137.5, respectively, thus suggesting that it is derived from three I3C molecules. However, the two methylene groups of DIM-1 resonated as singlets at δ_H 4.21 and 5.51, which were 1.3 ppm apart from each other. Such a chemical shift deviation of DIM-1 was much more pronounced than that (0.05 ppm) of LTr1 (δ_H 4.55 versus 4.50). Even more striking was the difference in the chemical shift of methylene carbons ($\delta_{C(DIM-1)}$ 41.4 and 21.1 versus $\delta_{C(LTr1)}$ 22.7 and 20.5). Along with the fifteen aromatic (vide supra) and

two imine proton signals (δ_H 9.90 and 11.18), the observation suggested that an indol-3-ylmethyl substituent had to anchor on the N1 site of an indole ring, whose C3 connecting to an indol-3-ylmethylene motif as discerned with LTr1 and DIM. In other words, the structure of DIM-1 was established as *N*-(indol-3-ylmethyl)-3,3'-diindolylmethane (Fig. 3).

In an analogous way, the fifth and sixth compounds, with R_t values of 10.047 and 12.036 min, respectively, was structurally elucidated to be *N*-(indol-3-ylmethyl)-indole-3-carbinol (I3C-1) (Fig. 3, S7, and S8) and *N*-(indol-3-ylmethyl)-indole-3-aldehyde (IAld-1) (Fig. 3, S9, and S10). The seventh compound (R_t = 12.983 min) was evidenced to have two indole rings as well one NH and a hydroxymethyl groups from its ^1H NMR spectrum. Further comparison with the spectrum of DIM indicated that it was *N*-hydroxymethyl-3,3'-diindolylmethane (DIM-2), unique in carrying an *N*-hydroxymethyl group (Fig. 3, S11, and S12). Collectively, our heat treatment showed that I3C was relatively stable at 60 and 80 °C. But, at 100 and 120 °C, I3C was oligomerized into DIM, CTr, LTr1, DIM-1, DIM-2, I3C-1 and IAld-1. This set of experimentation highlighted that I3C is heat-sensitive and can be converted upon heating into more diversified indoles under the physiological condition (near-neutral) than in the acidic context (Lin et al., 2022). Using these indoles as standards, we quantified the amount of I3C-1, IAld-1, DIM-1, and DIM-2 to be 4.6 ± 1.1, 0.4 ± 0.06, 3.1 ± 0.42, and 2.0 ± 0.02 μg/g in heated CVs (Table 1).

3.2. Prediction and synthesis of indoles in steamed CVs

The characterization of the heat-promoted I3C oligomers encouraged us to interrogate the driving force behind the transformation. Previously, we established the DIM formation from I3C through the formaldehyde-releasing dimerization pathway (Lin et al., 2022). Our substructure-based scrutiny of DIM, CTr, LTr1, DIM-1, DIM-2, I3C-1 and IAld-1 from the steamed CVs suggested that the heating process accelerated the Michael addition reaction of IAld, I3C and DIM with 3-
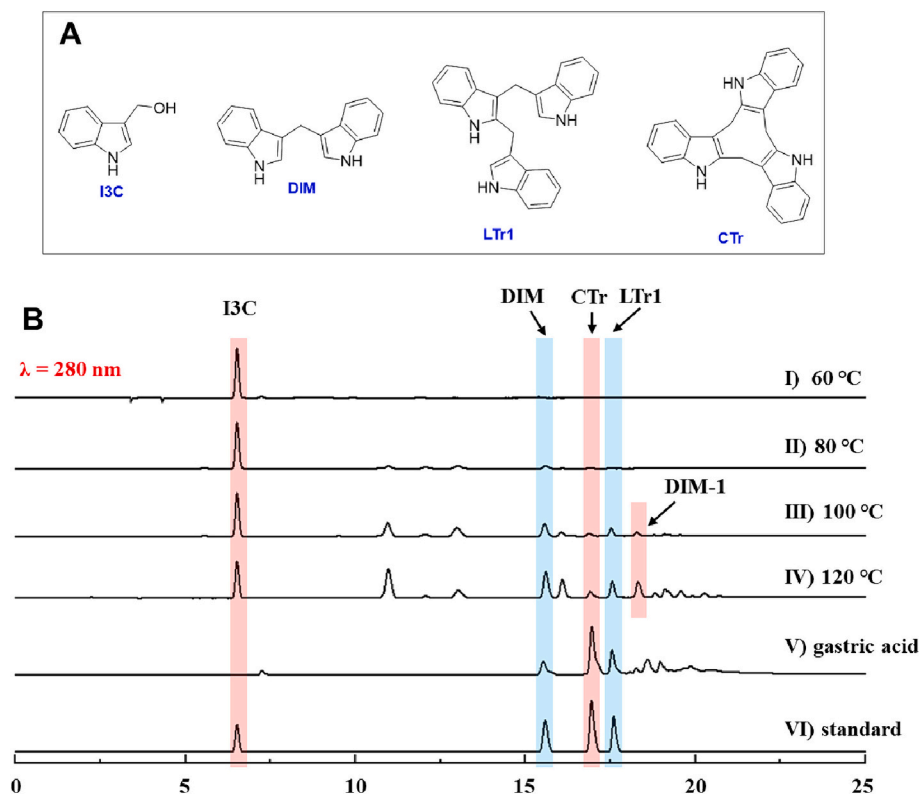
Fig. 2. Comparison of I3C derivatizations at different temperatures to the gastric acid-induced counterpart. (A) Structures of I3C, DIM, CTr and LTr1, which are well separated by HPLC (see entry VI in B). (B) HPLC profiles of products resulting from the 10-min treatment of I3C with gastric acid (V) or heated at 60 (I), 80 (II), 100 (III) and 120 °C (IV), respectively.
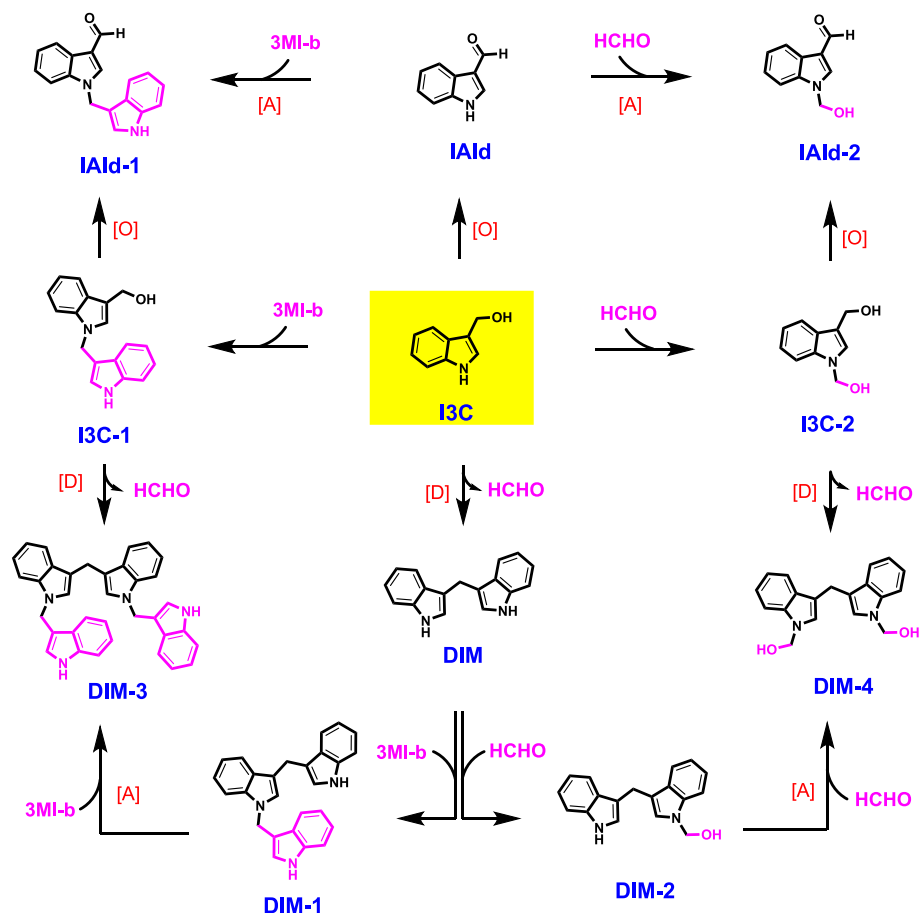
Fig. 3. The structures and putative pathway of the heat-promoted transformation of I3C. [A], [D] and [O] represent the alkylation, dimerization and oxidation reactions, respectively.

Table 1
The detection of *N*-substituted oligomers of I3C in cooked and fresh broccoli florets.

compounds	(μg/g) cooked broccoli $\pm$ SD	(μg/g) fresh broccoli $\pm$ SD
I3C-1	4.6 $\pm$ 1.1	ND
I3C-2	ND	ND
IAld-1	0.4 $\pm$ 0.06	ND
IAld-2	ND	ND
DIM-1	3.1 $\pm$ 0.42	ND
DIM-2	2.0 $\pm$ 0.02	ND
DIM-3	0.7 $\pm$ 0.08	ND
DIM-4	ND	ND

SD, standard deviation (n = 3); ND, not detected.

methyleneindole and formaldehyde formed therein (vide supra) (Fig. 3 and S3).

In acidic media, the C3 position of indoles seems to be more nucleophilic than the N1 atom (Fang, Li, Shi, Yao, & Lin, 2018), thereby explaining the regioselective (C3) bond formation involved in the gastric acid-promoted oligomerization of I3C. In contrast, this work identified the N-substituted indoles derived from I3C in CVs at their physiological pH around 6.5. Comprehensive rationalization of the present and previous observations (Fang et al., 2018) corroborated that the N1 nucleophilicity can be readily deprived by the salt formation in the presence of Lewis acid. However, in the present experimental setting, the N1 atom of IAld, I3C and DIM served as the nucleophilic sites to react with formaldehyde and 3-methyleneindole (Fig. 3 and S3).

The 'random reactions' between the three electrophiles and two nucleophiles mentioned above would provide a total of eight products (Fig. 3 and S3). Specifically, individual reactions of I3C and IAld with 3-methyleneindole generated *N*-indolemethyl-I3C (I3C-1) and *N*-indolemethyl-IAld (IAld-1), respectively. If reacting with formaldehyde, I3C and IAld should be converted to *N*-hydroxymethyl-I3C (I3C-2) and *N*-hydroxymethyl-IAld (IAld-2), respectively. However, DIM is di-nitrogenated and each nitrogen atom can attack at the electrophilic sites of 3-methyleneindole or formaldehyde to form *N*-indolemethyl-DIM (DIM-1), *N*-hydroxymethyl-DIM (DIM-2), *N,N'*-bis(indolemethyl)-DIM (DIM-3), and *N,N'*-bis(hydroxymethyl)-DIM (DIM-4) (Fig. 3). Gratifyingly, our first-round attempt led to the full characterization of structurally undescribed indoles (I3C-1, IAld-1, DIM-1 and DIM-2) generated from I3C and CVs upon heating (vide supra). Other predicted indoles (I3C-2, IAld-2, DIM-3, and DIM-4) failed to be isolated, presumably owing to their lower reaction probability since 3-methyleneindole or formaldehyde are in situ formed (vide supra) and can react with diverse nucleophiles in the reaction context if ignoring the heat-enhanced volatility of formaldehyde.

With the aim to probe whether I3C-2, IAld-2, DIM-3, and DIM-4 generated in the steamed CVs and to obtain enough amounts of I3C-1, IAld-1, DIM-1 and DIM-2 for biological evaluation, we sought out to synthesize them under the inspiration of the reported synthesis of I3C analogues (Huang, Yang, & He, 2022; Deguest, Bischoff, Fruit, & Marsais, 2007). As desired, I3C-2 and IAld-2 were respectively afforded through the *N*-hydroxymethylation of I3C and IAld with paraformaldehyde (Scheme S1). Such *N*-hydroxymethylation encouraged us to prepare DIM-2 and DIM-4 from DIM in yields of 67% and 91%, respectively, by tuning the paraformaldehyde amount in the reaction mixture (Scheme S1). With that, we were curious about whether IAld could be *N*-indol-3-ylmethylated into IAld-1, a less abundant I3C

daughter compound formed upon heating CVs (vide supra). However, we failed in the attempt presumably because the 3-methylene electrophilicity of 3MI-b could be weaker than the formaldehyde carbon. With IAld-2 in hand (vide supra), we tried to dehydrate IAld-2 into an indole-reactable indolium (Table S1) whose formation might be promoted by the elongation of the indole-based conjugation system. However, such attempts were terminated with failure, likely because IAld-2 refused to dehydrate in the given conditions (Table S1).

Next, we tried to address the frustration by taking the advantage of the ionic liquid (IL)-facilitated synthetic strategy that uses 1-ethyl-3-methylimidazolium chloride ([EMIm][Cl]) as a dual activator (Kumar et al., 2015). The chloride ion increased the N nucleophilicity of IAld via its hydrogen-bonding with the N—H proton, and the cationic ([EMIm]) part strengthened the 3-methylene electrophilicity of 3MI-b through its interaction with the N atom (Scheme 1A). Thus formed IL-substrate complex facilitated the IAld-1 synthesis in 47% yield through the IAld coupling with 3MI-b formed from I3C upon being kept at 120 °C for 1 h (Scheme 1B). Subsequently, the NaBH$_4$ reduction of IAld-1 gave I3C-1 in 93% yield, and the further coupling of I3C-1 with indole afforded DIM-1 in a 72% yield (Scheme 1B). Using SiO$_2$ as catalyst, I3C was transformed into DIM-3 through the formaldehyde-releasing dimerization pathway (Lin et al., 2022). With the authentic materials synthesized, we were able to confirm the heat-promoted generation of DIM-3 from indolyl glucosinolate embedded in fresh CV tissues (Table 1). Interestingly, the experiment allowed us to find the heat-intensified reverse reaction of *N*-hydroxymethylation. For example, as a hemiaminal, approximately one third of DIM-2 eliminated formaldehyde gradually to form DIM when kept at 100 °C for 1 h (Fig. S4). The observation explained why *N*-hydroxymethyl oligomers were (much) less abundant than *N*-(indol-3-yl)-methylated counterparts in the steamed broccoli florets (Table 1).

3.3. Anti-proliferation assay of heat-facilitated indoles

I3C and *N*-benzyl-I3C are inhibitory against the growth of human melanoma tumor (Kundu, Khouri, et al., 2017; Kundu, Quirit, Khouri, & Firstone, 2017). More recently, LTr1, a linear trimer of I3C, was demonstrated to kill the B16, WM115 and A375 melanoma cell lines, and in particular it enhances the melanoma-treating efficacy of chemotherapeutics (dacarbazine, vemurafenib and sorafenib) (Zhou, Liu, Qian, & Tan, 2022). With enough samples in hand, those reports motivated us to evaluate their biological activity of the *N*-alkylated indoles. Thus, all compounds obtained in the work were evaluated for the anti-proliferation efficacies against human melanoma cells. Among the *N*-substituted I3C oligomers, DIM-1 was found to be the most active against the A375 cells with (IC$_{50}$ value, 1.87 μM) (Fig. 4A and B). It demonstrated that DIM-1 was about 10-fold more effective than DIM (IC$_{50}$ value, >10 μM) against the growth of A375 cell lines with the magnitude comparable to that of LTr1 (IC$_{50}$ value, 1.40 μM) (Lin et al., 2022). In the long-term cell viability (colony formation) assay, DIM-1 at 0.5 μM was more effective against A375 cell than I3C at 5 μM (Fig. 4C and D).

CVs are drawing attention from academic and industrial communities for their nutritional value and pharmacological effects (González, Almanza, & Salcido, 2020). CVs are often consumed after being heated (e.g., boiling, blanching, steaming and stir-frying). Such cooking methods require high temperatures that render some CV chemicals transformed, thereby opening the possibility of improving taste, flavor and nutrient absorption (Pellegrini et al., 2010; Sun et al., 2021). Thermal breakdown of IGs had been widely investigated and a new minor indole condensation product 3-(indolylmethyl)glucobrassicin had been identified (Chevolleau et al., 2002). However, the chemistry governing heat-promoted conversion of I3C remains poorly investigated. Such knowledge gaps have motivated the present investigation to gain insights into the heat-facilitated direct transformation of I3C in steamed CVs into new types of indole derivatives. At a profile level, the indole products are distinct from the acidic pH-induced counterparts (Fig. 2B) (Lin et al., 2022). Furthermore, such indoles were produced in a temperature- and duration-dependent manner (Fig. 2B).
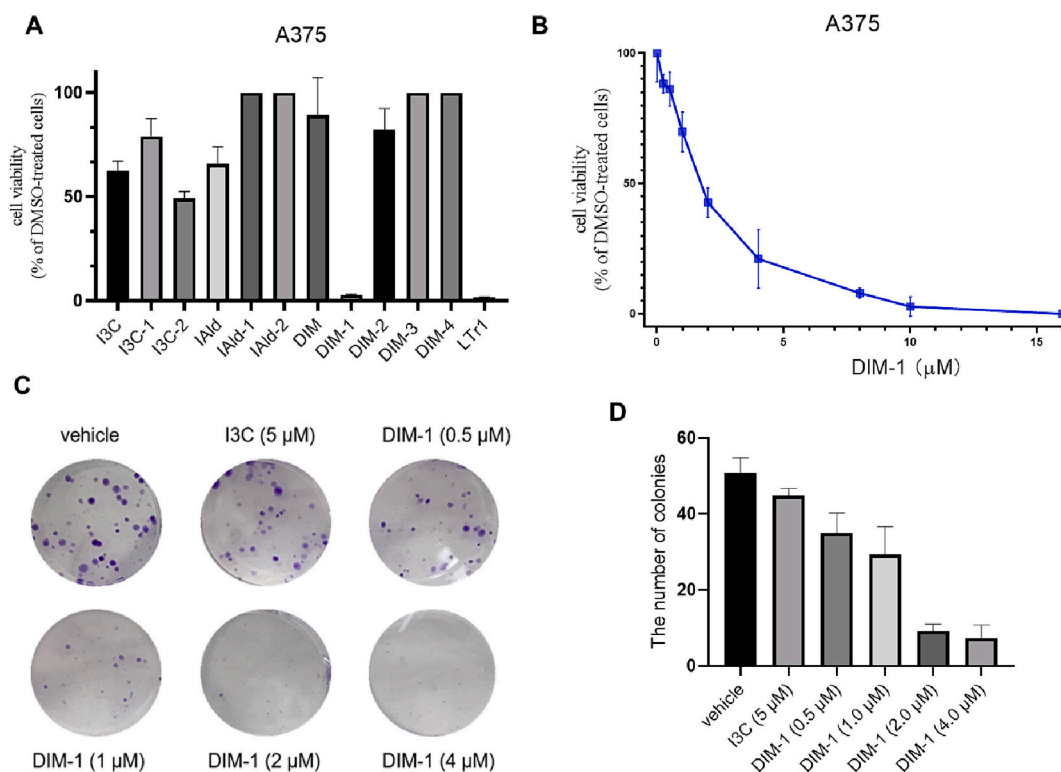
Fig. 4. Bio-evaluation of indoles obtained herein. (A) Anti-proliferation assay of I3C-derived oligomers at 10 μM against A375 cells. (B) The IC$_{50}$ value of DIM-1 ($n = 3$). (C and D) Colony formation assay of DIM-1 and I3C (n = 3).

To understand the determinant for the profile discrepancy, the indoles derived from I3C in different conditions were scrutinized at the substructural level. Unlike the acidic pH-induced derivatization of I3C (Lin et al., 2022), the heating process seems to favor the nucleophilic attack of imine N atoms of indole nuclei at diverse electrophiles including 3MI-b and formaldehyde formed in situ from the I3C dehydration and I3C-to-DIM dimerization, respectively (Fig. S3). The conclusion is further rationalized by CVs' physiological pH values around 6.5 (Fig. S2), which facilitate the generation of 3MI-b, but not 3MI-s, from the heat-promoted dehydration of I3C. Another in situ formed electrophile, formaldehyde, is a spin-off from the I3C dimerization into DIM as ascertained recently (Lin et al., 2022). Therefore, the near-neutral property of CVs plays key roles in keeping the imine N atoms nucleophilic enough to react with diverse electrophiles during the heating process.

According to the chemical logics reported (Fang et al., 2018), I3C-1 and I3C-2 could be air-oxidized into IAld-1 and IAld-2, and dimerized into DIM-3 and DIM-4 in the formaldehyde-releasing pathway (Fig. 3). However, the in situ formed formaldehyde and 3MI-b could react with other imine (NH)-bearing indoles such as LTr1 and CTr, thereby rendering the heat-facilitated I3C oligomerization more attractive for scientists working on or around the indole-related topic. In a broad sense, identification of dietary bioactive compounds is meaningful to gain insights into the relationship between diet and human health. However, under cooking, gastric acid, and/or gut bacteria, these molecules were transformed into metabolites with diverse structures, which accumulated in body and served as ultimate bioactive material. In continuation of our research on I3C as a CV-containing phytochemical (Lin et al., 2022; Liu et al., 2021; Qian et al., 2022; Zhu et al., 2021), we recognized that the electrophilicity of the indole N atom is retained at CVs' physiological pH (near-neutral). This observation, along with heat-processing, allowed for the production of arrays of *N*-substituted new indole molecules including DIM-1, a potent anti-proliferation agent present at 3.1 µg/g in cooked broccoli florets. With that, we may be encouraged to assume that the daily ingestion of cooked CVs could be beneficial for the prevention of melanoma, which has been ranked as the deadliest form of skin cancer with a poor prognosis (Zhou et al., 2022).

4. Conclusion

The cooking or heating process accelerated the direct conversion of I3C into indole derivatives, most of which are distinct from those resulting from the I3C transformations in acidic contexts. The key reason behind the discrepancy was dissected to be the near-neutral physiological pH that is supportive for the heat-promoted *N*-alkylation of indole nuclei of I3C and its oligomers by 3-methyleneindole (in the imine or base form) and formaldehyde formed in situ from the I3C dehydration and I3C-to-DIM conversion, respectively. Bio-evaluation of such *N*-alkylated indoles identified DIM-1 as an anti-proliferation indole found as concentrated as 3.1 µg/g in the steamed CVs. Taken together, the work updates the knowledge package about I3C and CVs by clarifying the heat-promoted derivatization of I3C in CVs into N-alkylated indoles, of which DIM-1 may serve as a lead compound valuable for the development of anti-proliferation agent(s).

CRediT authorship contribution statement

Jia Cheng Qian: Methodology, Investigation, Formal analysis, Data curation. **Heng Peng Zhang:** Methodology, Investigation, Formal analysis. **Yi Wang:** Validation, Investigation. **Dan Liu:** Writing – review & editing, Supervision, Project administration, Funding acquisition, Conceptualization.

Declaration of competing interest

The authors declare that they have no competing financial interests or personal relationships that could have appeared to influence the work reported in this paper.

Data availability

Data will be made available on request.

Appendix A. Supplementary data

Supplementary data to this article can be found online at https://doi.org/10.1016/j.fochx.2024.101410.

References

Anderton, M. J., Manson, M. M., Verschoyle, R. D., Gescher, A., Lamb, J. H., Farmer, P. B., … Williams, M. L. (2004). Pharmacokinetics and tissue disposition of indole-3-carbinol and its acid condensation products after oral administration to mice. *Clinical Cancer Research, 10*, 5233–5241. https://doi.org/10.1158/1078-0432.ccr-04-0163

Barnum, C. R., Cho, M. J., Markel, K., & Shih, P. M. (2024). Engineering Brassica crops to optimize delivery of bioactive products postcooking. *ACS Synthetic Biology, 13*, 736–744. https://doi.org/10.1021/acssynbio.3c00676

Blažević, I., Montaut, S., Burčul, F., Olsen, C. E., Burow, M., Rollin, P., & Agerbirk, N. (2020). Glucosinolate structural diversity, identification, chemical synthesis and metabolism in plants. *Phytochemistry, 169*, Article 112100. https://doi.org/10.1016/j.phytochem.2019.112100

Chevolleau, S., Debrauwer, L., Boyer, G., & Tulliez, J. (2002). Isolation and structure elucidation of a new thermal breakdown product of glucobrassicin, the parent indole glucosinolate. *Journal of Agriculture and Food Chemistry, 50*, 5185–5190. https://doi.org/10.1021/jf020125i

Choe, U., Yu, L. L., & Wang, T. T. Y. (2018). The science behind microgreens as an exciting new food for the 21st century. *Journal of Agriculture and Food Chemistry, 66*, 11519–11530. https://doi.org/10.1021/acs.jafc.8b03096

Deguest, G., Bischoff, L., Fruit, C., & Marsais, F. (2007). Anionic, in situ generation of formaldehyde: A very useful and versatile tool in synthesis. *Organic Letters, 9*(6), 1165–1167. https://doi.org/10.1021/ol070145b

Dong, M. Y., Tian, Z. H., Ma, Y. N., Yang, Z. Y., Ma, Z., Wang, X. M., … Jiang, H. Q. (2021). Rapid screening and characterization of glucosinolates in 25 Brassicaceae tissues by UHPLC-Q-exactive orbitrap-MS. *Food Chemistry, 365*, Article 130493. https://doi.org/10.1016/j.foodchem.2021.130493

Fang, X. X., Li, Q. Y., Shi, R., Yao, H. Q., & Lin, A. J. (2018). Controllable Pd-catalyzed allylation of indoles with skipped enynes: Divergent synthesis of indolenines and N-allylindoles. *Organic Letters, 20*, 6084–6088. https://doi.org/10.1021/acs.orglett.8b02481

Fujioka, N., Waldman, C. E. A., Upadhyaya, P., Carmella, S. G., Fritz, V. A., Rohwer, C., … S. S.. (2014). Urinary 3,3'-Diindolylmethane: A biomarker of glucobrassicin exposure and indole-3-carbinol uptake in humans. *Cancer Epidemiology, Biomarkers & Prevention, 23*(2), 282–287. https://doi.org/10.1158/1055-9965.epi-13-0645

González, K. M. F., Almanza, A. Y. H., & Salcido, N. M. F. (2020). The value of bioactive compounds of cruciferous vegetables (Brassica) as antimicrobials and antioxidants: A review. *Journal of Food Biochemistry, 00*, Article e13414. https://doi.org/10.1111/jfbc.13414

Gronke, K., Hernández, P. P., Zimmermann, J., Klose, C. S. N., Kofoed-Branzk, M., Guendel, F., … Diefenbach, A. (2019). Interleukin-22 protects intestinal stem cells against genotoxic stress. *Nature, 566*, 249–253. https://doi.org/10.1038/s41586-019-0899-7

Huang, W. B., Yang, M., & He, L. N. (2022). Metal-free hydroxymethylation of indole derivatives with formic acid as an alternative way to indirect utilization of CO2. *The Journal of Organic Chemistry, 87*, 3775–3779. https://doi.org/10.1021/acs.joc.1c02831

Johnson, I. T. (2018). Cruciferous vegetables and risk of cancers of the gastrointestinal tract. *Molecular Nutrition & Food Research, 62*, 1701000. https://doi.org/10.1002/mnfr.201701000

Kokotou, M. G., Revelou, P. K., Pappas, C., & Kokotou, V. C. (2017). High resolution mass spectrometry studies of sulforaphane and indole-3-carbinol in broccoli. *Food Chemistry, 237*, 566–573. https://doi.org/10.1016/j.foodchem.2017.05.139

Kumar, R., Saima, R., Shard, A., Andhare, N. H., Richa, N. H., & Sinha, A. K. (2015). Thiol–ene "click" reaction triggered by neutral ionic liquid: The "ambiphilic" character of [hmim]Br in the regioselective nucleophilic hydrothiolation. *Angewandte Chemie International Edition, 54*(3), 828–832. https://doi.org/10.1002/anie.201408721

Kundu, A., Khouri, M. G., Aryana, S., & Firstone, G. L. (2017). 1-benzyl-indole-3-carbinol is a highly potent new small molecule inhibitor of Wnt/β-catenin signaling in melanoma cells that coordinately inhibits cell proliferation and disrupts expression of microphthalmia-associated transcription factor isoform-M. *Carcinogenesis, 38*(12), 1207–1217. https://doi.org/10.1093/carcin/bgx103

Kundu, A., Quirit, J. G., Khouri, M. G., & Firstone, G. L. (2017). Inhibition of oncogenic BRAF activity by indole-3-carbinol disrupts microphthalmia-associated transcription

factor expression and arrests melanoma cell proliferation. *Molecular Carcinogenesis, 56*, 49–61. https://doi.org/10.1002/mc.22472

Kus, J., & Misz-Kennan, M. (2017). Coal weathering and laboratory (artificial) coal oxidation. *International Journal of Coal Geology, 171*, 12–36. https://doi.org/10.1016/j.coal.2016.11.016

Lee, S. Y., Liang, Y. N., Stuckey, D. C., & Hu, X. (2023). Single-step extraction of bioactive compounds from cruciferous vegetable (kale) waste using natural deep eutectic solvents. *Separation and Purification Technology, 317*, Article 123677. https://doi.org/10.1016/j.seppur.2023.123677

Lee, Y. R., Chen, M., Lee, J. D., Zhang, J. F., Lin, S. Y., Fu, T. M., … Pandolfi, P. P. (2019). Reactivation of PTEN tumor suppressor for cancer treatment through inhibition of a MYC-WWP1 inhibitory pathway. *Science, 364*, eaau0159. https://doi.org/10.1126/science.aau0159

Li, N., Wu, X. T., Zhuang, W., Wu, C. C., Rao, Z. Y., Du, L., & Zhou, Y. (2022). Cruciferous vegetable and isothiocyanate intake and multiple health outcomes. *Food Chemistry, 375*, Article 131816. https://doi.org/10.1016/j.foodchem.2021.131816

Lin, L. P., Liu, D., Qian, J. C., Wu, L., Zhao, Q., & Tan, R. X. (2022). Post-ingestion conversion of dietary indoles into anticancer agents. *National Science Review, 9*, nwab144. https://doi.org/10.1093/nsr/nwab144

Lin, L. P., Yu, H. Y., Shi, J., Zhou, Z. Z., & Tan, R. X. (2023). Gene-directed generation of unprecedented bioactive compounds. *ACS Sustainable Chemistry & Engineering, 11*, 6619–6628. https://doi.org/10.1021/acssuschemeng.2c07708

Lin, L. P., Yuan, P., Jiang, N., Mei, Y. N., Zhang, W. J., Wu, H. M., … Tan, R. X. (2015). Gene-inspired mycosynthesis of skeletally new indole alkaloids. *Organic Letters, 17*, 2610–2613. https://doi.org/10.1021/acs.orglett.5b00882

Liu, D., Jiang, N., Huang, W. D., Li, J. W., Zhu, W. J., & Tan, R. X. (2021). Ionic-liquid-catalyzed access to CTr: An antitumor agent. *ACS Sustainable Chemistry & Engineering, 9*, 5138–5147. https://doi.org/10.1021/acssuschemeng.1c00191

Lyles, J. T., Luo, L. P., Liu, K., Jones, D. P., Jones, R. M., & Quave, C. L. (2021). Cruciferous vegetables (Brassica oleracea) confer cytoprotective effects in Drosophila intestines. *Gut Microbes, 13*(1), 1921926. https://doi.org/10.1080/19490976.2021.1921926

Mikkelsen, M. D., Buron, L. D., Salomonsen, B., Olsen, C. E., Hansen, B. G., Mortensen, U. H., & Halkier, B. A. (2012). Microbial production of indolylglucosinolate through engineering of a multi-gene pathway in a versatile yeast expression platform. *Metabolic Engineering, 14*, 104–111. https://doi.org/10.1016/j.ymben.2012.01.006

Nagia, M., Morgan, I., Gamel, M. A., & Farag, M. A. (2023). Maximizing the value of indole-3-carbinol, from its distribution in dietary sources, health effects, metabolism, extraction, and analysis in food and biofluids. *Critical Reviews in Food Science and Nutrition*. https://doi.org/10.1080/10408398.2023.2197065. ahead of print.

Niels, A., Martin, D. V., & Jae, H. K. (2009). Indole glucosinolate breakdown and its biological effects. *Phytochemistry Reviews, 8*, 101–120. https://doi.org/10.1007/s11101-008-9098-0

Pellegrini, N., Chiavaro, E., Gardana, C., Mazzeo, T., Contino, D., Gallo, M., … Porrini, M. (2010). Effect of different cooking methods on color, phytochemical concentration, and antioxidant capacity of raw and frozen brassica vegetables. *Journal of Agricultural and Food Chemistry, 58*, 4310–4321. https://doi.org/10.1021/jf904306r

Qian, J. C., Liu, D., Lin, L. P., Zhu, W. J., & Tan, R. X. (2022). Minor bioactive indoles from kimchi mirror the regioselectivity in indole-3-carbinol oligomerization. *Food Chemistry, 382*, Article 132571. https://doi.org/10.1016/j.foodchem.2022.132571

Sun, J., Wang, Y. F., Pang, X. Y., Tian, S. H., Hu, Q. B., Li, X. F., … Lu, Y. J. (2021). The effect of processing and cooking on glucoraphanin and sulforaphane in brassica vegetables. *Food Chemistry, 360*, Article 130007. https://doi.org/10.1016/j.foodchem.2021.130007

Wen, Z., Yang, K. C., Deng, J. F., & Chen, L. (2023). Advancements in the preparation of 4*H*-Chromenes: An overview. *Advanced Synthesis & Catalysis, 365*(9), 1290–1331. https://doi.org/10.1002/adsc.202201409

Xu, D. H., Lin, J. H., Sun, S. C., Ma, R., Wang, M. L., Yang, J. L., & Luo, J. (2022). Microwave pyrolysis of biomass model compounds for bio-oil: Formation mechanisms of the nitrogenous chemicals and DFT calculations. *Energy Conversion and Management, 262*, Article 115676. https://doi.org/10.1016/j.enconman.2022.115676

Zhou, B. B., Liu, D., Qian, J. C., & Tan, R. X. (2022). Vegetable-derived indole enhances the melanoma-treating efficacy of chemotherapeutics. *Phytotherapy Research, 36*, 4278–4292. https://doi.org/10.1002/ptr.7565

Zhu, W. J., Lin, L. P., Liu, D., Qian, J. C., Zhou, B. B., Yuan, D. D., & Tan, R. X. (2021). Pharmacophore-inspired discovery of FLT3 inhibitor from kimchi. *Food Chemistry, 361*, Article 130139. https://doi.org/10.1016/j.foodchem.2021.130139